

Symmetry-breaking effects and spontaneous generation of vortices in hybrid superconductor-ferromagnet nanostructures

Qinghua Chen,¹ Carlos Carballeira,^{1,2,*} and Victor V. Moshchalkov¹¹*INPAC-Institute for Nanoscale Physics and Chemistry, K. U. Leuven, Nanoscale Superconductivity and Magnetism & Pulsed Fields Group, Celestijnenlaan 200 D, 3001 Leuven, Belgium*²*LBTS, Departamento de Física da Materia Condensada, Universidade de Santiago de Compostela, Santiago de Compostela E-15782, Spain*

(Received 20 September 2006; published 28 December 2006)

By using the nonlinear Ginzburg-Landau equations, we investigate symmetry-breaking effects at temperatures well below the normal-superconducting phase boundary, $T_c(H)$, in a superconducting microsquare with a magnetic dot on top under a perpendicular magnetic field. Vorticity values forbidden by the inhomogeneous field of the dot at $T_c(H)$ are progressively recovered deep inside the superconducting state. This restoration of the increase of the fluxoid quantum number by 1 with decreasing temperature is achieved both by the conventional flux expulsion and by the spontaneous generation of additional vortices. The associated transitions between vortex states can be detected experimentally by measuring the temperature dependence of the magnetization.

DOI: [10.1103/PhysRevB.74.214519](https://doi.org/10.1103/PhysRevB.74.214519)

PACS number(s): 74.78.Na, 74.20.De, 74.25.Dw, 75.75.+a

I. INTRODUCTION

Quantization effects associated with the confinement of superconducting condensate at length scales of the order of the superconducting coherence length, $\xi(T)$, have been studied since more than three decades ago.¹⁻³ The interest in this issue has been considerably enhanced in the last years by advances in micro- and nanofabrication techniques that make possible the design of submicron superconducting structures with *ad hoc* shape. In these superconductors both the critical parameters and the vortex matter change substantially with respect to the reference behavior of the bulk materials.⁴⁻⁶ A good example here is the normal-superconducting phase boundary [$T_c(H)$] of a submicron structure that shows a cusplike behavior superimposed with a linear background. Close to $T_c(H)$ the vortices do not order themselves in a triangular vortex lattice. Instead, they form vortex patterns consistent with the geometry of the sample, so that superconductivity nucleates in the form of a giant vortex at the center of mesoscopic disks^{2,3} and vortex-antivortex pairs can be spontaneously generated in structures with discrete symmetry.⁷⁻¹¹

However, these symmetry-induced effects are expected to disappear deep inside the superconducting phase, where the nonlinear effects related to the nonlinear term of the Ginzburg-Landau (GL) equations cannot be ignored. Therefore the stability of the symmetric vortex patterns at $T_c(H)$ is a crucial issue both from the experimental and technological point of view that has been already addressed for different geometries of individual superconducting microstructures.¹²⁻²² It has been found that the nucleated order parameter, including the vortex-antivortex patterns in triangles and squares, is stable in broad field-temperature regions that can be enlarged by decreasing the sample size,¹⁶⁻²¹ and enforced by artificial pinning.²² However, deep inside the superconducting phase it undergoes different symmetry-switching and symmetry-breaking transitions that lead to a progressive recovery of the Abrikosov vortex lattice.

Recently, we have applied the linearized GL (LGL) theory to study the hybrid superconducting-ferromagnet (SF) nanostructure consisting of a magnetic dot on top of a superconducting microsquare.²³ We have found that the dot induces an expansion of the symmetry consistent vortex-antivortex patterns and multiquanta vortex entries along $T_c(H)$, two findings which are well beyond the expected behavior of the superconducting square itself. The aim of this work is to investigate, by using the full nonlinear GL functional, the symmetry breaking effects induced by decreasing temperature in the same SF nanostructure. We show that the behavior of the SF-system inside the superconducting phase also strongly differs from that of an individual microsquare. In particular, we observe that the usual increment of the fluxoid quantum number (also called vorticity, L) by 1, broken close to $T_c(H)$ due to the multiquanta vortex entries, is restored deeper in the superconducting state. One of the mechanisms of this recovery of L -values is the flux expulsion at low temperatures already observed in individual microsuperconductors,^{12,13,16-21} but we have also found that in this SF nanostructure vortices can be spontaneously generated by decreasing temperature. These changes in the vorticity are associated with transitions between vortex patterns that may give rise to measurable effects in the increment of the magnetization with varying the temperature.

II. METHOD OF SOLUTION

The linearized Ginzburg-Landau theory has been probed as an adequate tool to describe the properties of microsuperconductors close to $T_c(H)$;^{1-7,10,21,23} a region of the phase-diagram where the amplitude of the superconducting order parameter, $|\Psi|$, may be considered small. However, this assumption is no longer valid deeper in the superconducting state and, subsequently, the fourth power term in $|\Psi|$ has to be included in the free energy expansion. The resulting nonlinear GL-functional may be written as²⁴

$$F = F_n + \int \left[\Psi^* \hat{L} \Psi + \alpha |\Psi|^2 + \beta |\Psi|^4 + \frac{(\vec{h} - \vec{H})^2}{8\pi} \right] d\vec{r}, \quad (1)$$

where F_n is the energy of the normal state, $\hat{L} = (-i\hbar\vec{\nabla} - \frac{2\pi}{\phi_0}\vec{A})^2/2m^*$ is the linearized GL operator, ϕ_0 is the magnetic flux quantum, \vec{A} is the vector potential, α and β are the GL parameters, and \vec{h} and \vec{H} are, respectively, the local and applied magnetic fields. In the case of a microsquare with a magnetic dot on top, Eq. (1) has to be solved by taking into account both the superconductor-vacuum boundary condition,²⁴

$$\left(\frac{\hbar\vec{\nabla}}{i} - \frac{2\pi}{\phi_0}\vec{A} \right) \Psi|_n = 0 \quad (2)$$

(here n holds for the normal to the boundary line) and the dot contribution to the external magnetic field. For a disk-shaped dot, magnetized parallel to the z -direction, the latter can be obtained from magnetostatic calculations as²⁵

$$A_\varphi^{dot} = 4M_{dot} \sqrt{\frac{R}{r}} \int_0^l dz_d \frac{\left[\left(1 - \frac{k^2}{2} \right) K(k) - E(k) \right]}{k}, \quad (3)$$

with $A_r^{dot} = A_z^{dot} = 0$. In Eq. (3) K and E are, respectively, the elliptic integrals of the first and second kind and r is the radial coordinate. The magnetization, radius, and length of the dot are denoted by, respectively, M_{dot} , R , and l , while the dimensionless variable $k^2 = 4Rr / [(R+r)^2 + (z-z_d)^2]$ includes the z -dependence of A_φ^{dot} . For simplicity and better comparison with our previous results on the nucleated properties of the same system, in our present calculations we have employed the same dot parameters as in Ref. 23, namely, $M_{dot} = 18\phi_0$, $R = 0.4a$, $l = 0.033a$, and $z = -0.0025a$ (here a stands for the length of the microsquare). The latter accounts for the thickness of a substrate separating the superconductor from the magnetic dot in order to avoid proximity effects. Note also that these parameters are similar to those of the magnetic dots used in different hybrid SF nanostructures already studied experimentally.²⁶ The presence of an external homogeneous field is taken into account by adding $A_\varphi^{ext} = Hr/2$ to Eq. (3).

To simplify the minimization of Eq. (1) under both Eqs. (2) and (3), in what follows we will assume the case of a microsquare with dimensions, thickness d and size a , satisfying both $d \ll \xi(T)$ and $d, a \ll \lambda(T)$ [here $\lambda(T)$ is the superconducting penetration depth]. The first condition warrants that the order parameter will be constant across the thickness of the square and, subsequently, Eq. (1) can be solved in two dimensions. Under the second assumption the distortion of the magnetic field inside the superconductor due to the presence of screening currents may be discarded. The local field will then coincide with the external field, and the magnetic energy term in Eq. (1) can be neglected. At the same time, the vector potential will not be coupled to the superconducting order parameter, so that the minimization of the free energy functional has to be performed only with respect to Ψ . It is then convenient to perform an expansion of the su-

perconducting order parameter by using the eigenfunctions of the linear problem, $\hat{L}\phi_i = \epsilon_i\phi_i$ (ϵ_i being the eigenvalue corresponding to the eigenfunction ϕ_i), as a basis set. If we write this expansion as $\Psi = \sum_i c_i \phi_i$, where c_i are complex coefficients, Eq. (1) is transformed into^{13,18,19,21}

$$(F - F_n)\beta = \sum_i (\alpha + \epsilon_i) c_i^* c_i + \frac{1}{2} \sum_{ijkl} A_{ij}^{kl} c_i^* c_j^* c_k^* c_l^*. \quad (4)$$

In the above expression $c_i' = \sqrt{\beta} c_i$ and $A_{ij}^{kl} = \int \phi_i^* \phi_j^* \phi_k \phi_l d\vec{r}$ are the coefficients that, together with ϵ_i , govern the admixture between the different solutions of the LGL equation.^{13,18,19,21} Note that the renormalization of the c_i coefficients removes any β -dependence from the right-hand side of Eq. (4). Therefore its solutions will be independent of the choice of κ and applicable for both type-I and type-II superconductors.

Provided that the solutions of the linear part are obtained while taking into account Eqs. (2) and (3), the problem of solving the full GL-functional for a microsquare with a magnetic dot on top is reduced to find the c_i' -coefficients that minimize Eq. (4). Therefore we have solved the LGL equation following the procedure described previously for individual superconducting micropolygons under a homogeneous applied field,^{7,10,21,27} that is based on a gauge transformation of the vector potential that converts Eq. (2) into the Neumann boundary condition, $\nabla\Psi|_n = 0$. The field-dependent ϕ_i -eigenvalues may be then calculated by using an analytic basis set, and they can be classified within the irreducible representations (irreps) of the symmetry group of the problem. For a fourfold symmetry, these irreps are denoted as A , B , $E+$, and $E-$ and they are characterized by having, respectively, no vortex ($L=0$), a giant vortex ($L=+2$), one vortex ($L=+1$), and one antivortex ($L=-1$) at the center of the sample. The same approach can be adapted to take into account the presence of the inhomogeneous field produced by a cylindrically symmetric magnetic dot on top of the microsuperconductor.²³ However, the relative complexity of Eq. (3) makes difficult the integration of the differential equations required to perform the gauge transformation of the vector potential (see Refs. 21 and 27). To avoid these complications, we have approximated A_φ^{dot} by rational functions, using as many terms as necessary to reproduce well the field profile resulting from Eq. (3) for a given set of dot parameters.

The present calculations have been performed by using 24 functions in the Ψ -expansion that correspond to the six lowest energy levels of each irrep. Nevertheless, we have checked that, in the range of studied temperatures and fields, no difference is observed in the final results by using larger sets of functions. For the minimization of Eq. (4) we have chosen a Monte Carlo method with a Mersenne algorithm for the generation of random numbers. We have also used the continuity of the free energy as a function of the temperature and the magnetic field to discard metastable solutions.

III. RESULTS AND DISCUSSION

The positive values of the vorticity (calculated from $\oint \vec{\nabla}\varphi \cdot d\vec{l} = 2\pi L$, where φ is the phase of the order parameter

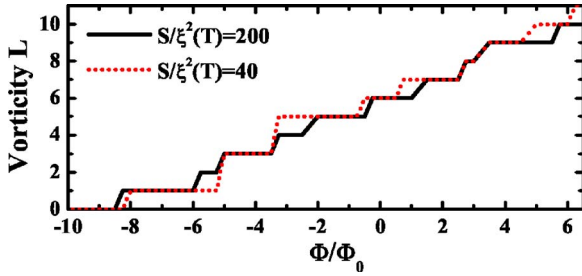


FIG. 1. (Color online) Applied magnetic flux dependence of the positive values of the vorticity of the sample at two different temperatures. Close to $T_c(H)$, at $S/\xi^2(T)=40$, L changes by +2 from 1 to 3 and from 3 to 5, but deeper in the superconducting phase, for $S/\xi^2(T)=200$, the increment of the vorticity by 1 is restored. However, $L=4$ is recovered by expelling a flux quantum from the sample, while to obtain $L=2$ a vortex is spontaneously nucleated at decreasing temperature.

and the integration is carried out along the sample's boundary²⁴) at two different temperatures [given in units of $S/\xi^2(T)$, $S=a^2$ being the square's area] are presented in Fig. 1 as a function of ϕ/ϕ_0 , where $\phi=H \cdot S$ is the applied magnetic flux. Close to the normal-superconducting transition, at $S/\xi^2(T)=40$ (red dotted line), the same multi-quanta vortex entries, found at $T_c(H)$ in Ref. 23, are seen. In particular, this curve reveals jumps in L from 1 to 3 at $\phi/\phi_0 \approx -5$ and from 3 to 5 at $\phi/\phi_0 \approx -3.25$, both indicating the simultaneous entry of two flux quanta in the sample. However, when the temperature is lowered down to $S/\xi^2(T)=200$ (black line) the states with $L=2$ and $L=4$ are restored. This effect may be intuitively understood in terms of the decrease of $\xi(T)$,

allows faster spatial variations of the order parameter (including smaller vortex cores) that may overcome the inhomogeneity of the field of the dot. Figure 1 also suggests two different mechanisms for the recovery of these L values. Note that at a magnetic field of the order of $\phi/\phi_0 \approx -2.5$ the vorticity changes from 5 to 4 when going from $S/\xi^2(T)=40$ to $S/\xi^2(T)=200$, a decrease of the fluxoid quantum number with lowering the temperature already observed in individual microsuperconductors.^{12,13,16-21} Instead, for $\phi/\phi_0 \approx -5.5$ the L value unexpectedly *increases* from 1 to 2 with decreasing the temperature, which corresponds to a counterintuitive spontaneous generation of a vortex.

The nucleation of a vortex with decreasing temperature observed in Fig. 1 is schematically depicted in Fig. 2, where in panels (a)–(c) the spatial distribution of $|\Psi|$ in the square (higher values in red) is presented for three different temperatures under a magnetic field of $\phi/\phi_0 = -5.25$. The dotted circumference indicates the region below the dot. For completeness, panel (d) shows a zoom around $\phi/\phi_0 = -5.25$ of the magnetic field dependence of the energy [in $S/\xi^2(T)$ units] of the three first Landau levels of each irrep involved in the Ψ -expansion. When compared with the energy spectrum of an individual microsquare,^{18,21} this figure illustrates that the presence of the dot leads to much smaller differences between the lowest Landau levels (LLL) of the irreps. Thus close to $T_c(H)$ [panel (a)] the vortex pattern is still determined by the irrep with lowest energy, $E+$, and it consists of a single vortex placed at the center of the square. However, with decreasing temperature this solution is being admixed with the LLL of the other three irreps, which leads to the nucleation of a second vortex in one side of the square that is attracted to the center by the dot [panel (b)]. This type of

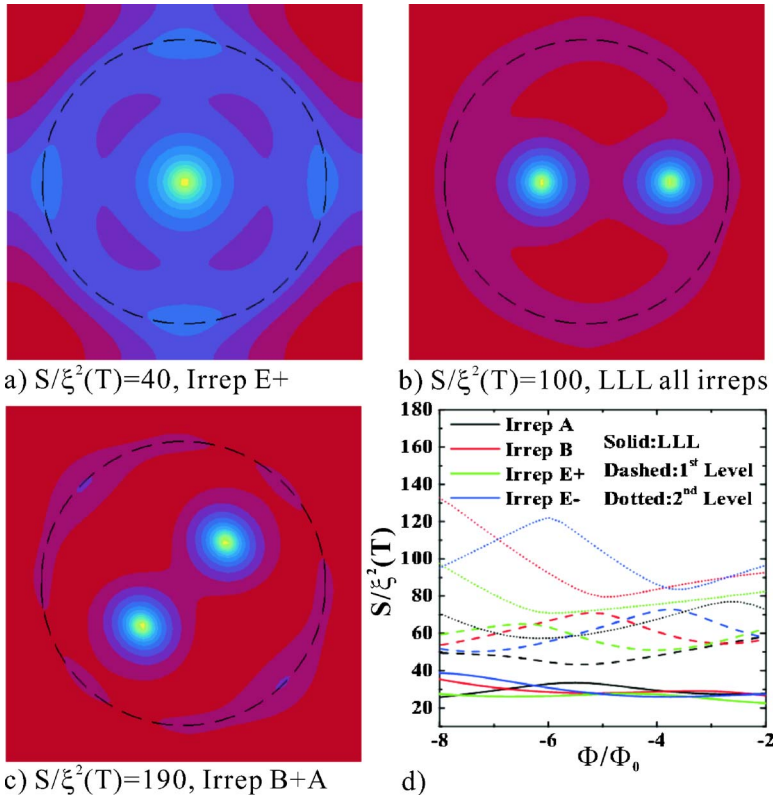


FIG. 2. (Color online) (a)–(c) Sequence of the $1 \rightarrow 2 \rightarrow 2$ transition between vortex states at $\phi/\phi_0 = -5.25$, which involves the nucleation of an extra vortex with decreasing temperature. Panel (d) presents a zoom around this flux-value of the field dependence of the three first energy levels of each irrep in the Ψ expansion. The generation of the second vortex arises from the admixture of the nucleated order parameter (LLL of irrep E+) with the ground state of the other three irreps which, as shown by (d), have similar energy.

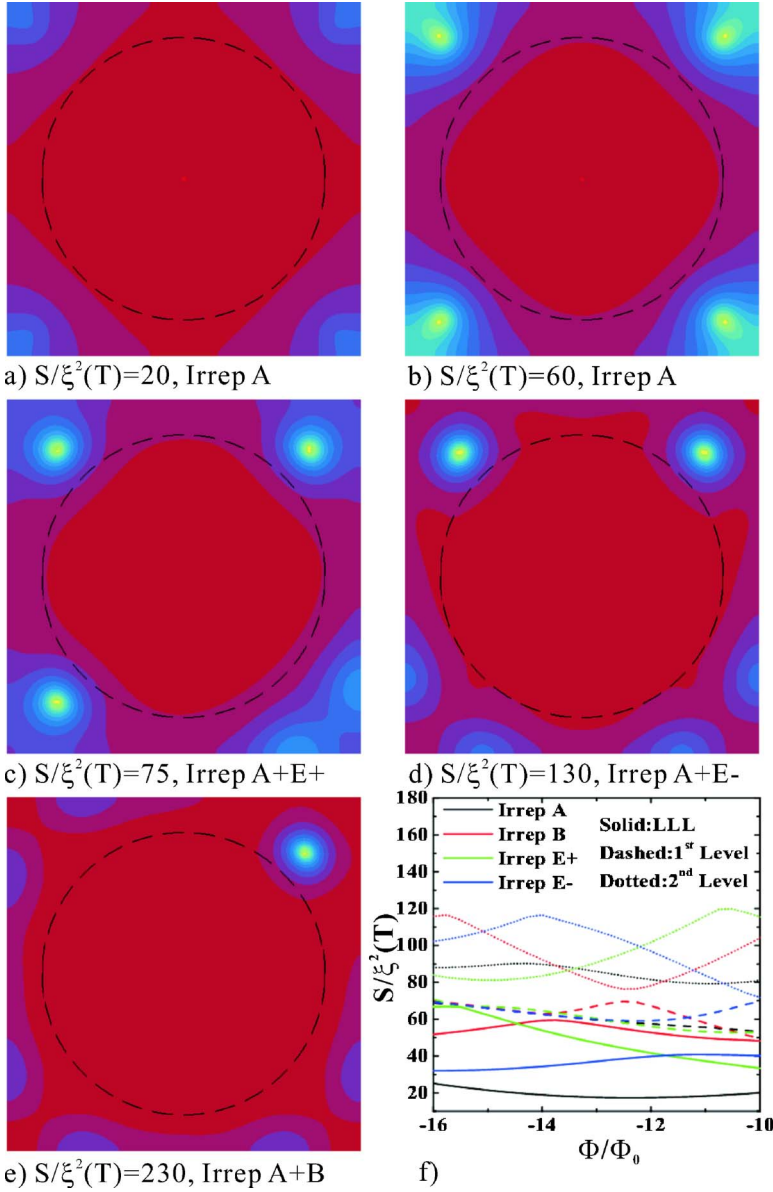


FIG. 3. (Color online) (a)–(e) Sequence of the $0 \rightarrow -4 \rightarrow -3 \rightarrow -2 \rightarrow -1$ transitions between vortex states at $\phi/\phi_0 = -12.8$. Panel (f) shows a zoom around this flux value of the field dependence of the energy of the three first Landau levels of each irrep. When the temperature decreases L first changes from 0 to -4 (a \rightarrow b) by spontaneously nucleating four antivortices at the corners of the square. Deeper in the superconducting phase, these antivortices are progressively expelled from the sample, leading to the recovery of the L -values -3 , -2 , and -1 (c \rightarrow e) absent at the boundary. However, due to the small energy differences between the levels involved in this process (LLL of irrep B and first excited levels of irreps $E+$ and $E-$), this restoration of the negative L -values will be very sensitive to small perturbations.

admixture has not been found in the microsquare itself, where symmetry-breaking transitions between vortex states arise from the admixture of the ground state of one irrep with one or more excited levels of the others.^{18,21} This last situation is recovered deeper in the superconducting phase [panel (c)], where the two vortices arrange themselves along one of the diagonals of the square. This configuration results, analogously to the breaking of the giant vortex state of an individual microsquare,^{18,21} from the admixture of the LLL of irrep B with the first excited level of irrep A .

The spontaneous nucleation of vortices when cooling down also occurs for negative L -values and it can involve more than one single flux quantum. To illustrate these points, in Fig. 3 the evolution of the Ψ -distribution in the square with decreasing temperature is presented at $\phi/\phi_0 = -12.8$ [panels (a)–(e)] together with a zoom around this flux value of the magnetic field dependence of the energy of the three first Landau levels of each irrep [panel (f)]. The nucleated order parameter [Fig. 3(a)] corresponds to a solution with

$L=0$; but when the temperature decreases four antivortices (that we define as flux lines antiparallel to the magnetization of the dot) are simultaneously nucleated at the corners of the square [Fig. 3(b)], where they stay as a consequence of the dot repulsion. Deeper into the superconducting phase these antivortices are progressively expelled from the square, an effect already observed in individual microsquares^{18,21} that in this hybrid SF structure results in a recovery of the L -values -3 , -2 , and -1 absent at $T_c(H)$.²³ We have found that the spontaneous nucleation of the four antivortices arises from an admixture of the LLL of irrep A with the two first excited levels of the same irrep. When the temperature is further decreased, this combination admixes with the LLL of irrep B and the first excited states of irreps $E+$ and $E-$. The resulting nonsymmetric vortex pattern is then determined by the level among these three with the highest $|c'_i|$ in the Ψ -expansion, namely, irrep $E+$ first excited level for $L=-3$ [Fig. 3(c)], irrep $E-$ first excited level for $L=-2$ [Fig. 3(d)], and irrep B LLL for $L=-1$ [Fig. 3(e)]. However, these coefficients are

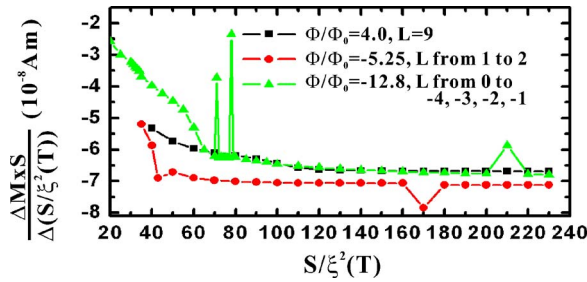


FIG. 4. (Color online) Temperature dependence of the differential magnetization for $\phi/\phi_0=4$ and the two magnetic fields studied in Figs. 2 and 3. For both $\phi/\phi_0=-5.25$ and -12.8 the curves show peaks around the transition points between different vortex states [$S/\xi^2(T) \approx 42$ and 170 and, respectively, $S/\xi^2(T) \approx 72, 79$, and 220]. Instead, for $\phi/\phi_0=4$ we have observed a stable vortex pattern with $L=9$ and the differential magnetization shows no critical behavior.

very similar since, as shown by Fig. 3(f), the levels also have similar energies. As a consequence, in contrast to the spontaneous generation of the four vortices, the progressive expulsion of flux lines at low temperatures seems to be an unstable process that will be very sensitive to small perturbations. This instability affects broad field regions corresponding to negative vorticities. Therefore only the recovery of positive L -values is presented in Fig. 1.

The transitions between vortex states with decreasing temperature can be related with either a jump or a smooth increase of the c'_i -coefficients of the admixed states.^{18,19,21} In the first case, such critical behavior may give rise to measurable effects in different observables, such as the magnetization, thus providing new possibilities to investigate the superconducting phase of mesoscopic superconductors. This is illustrated by Fig. 4, where the temperature dependence of the differential magnetization, $\Delta M \times S / \Delta[S/\xi^2(T)]$ is presented for $\phi/\phi_0=4$ and the two magnetic fields studied in Figs. 2 and 3. To obtain these curves we have used $M = \frac{1}{2c_S} \int_S \vec{r} \times \vec{j}$ (here \vec{j} is the supercurrent) for the averaged magnetization. It is clearly seen that for $\phi/\phi_0=-5.25$ the differential magnetization shows jumps at the temperatures at which the vortex induced by decreasing temperature is generated [$S/\xi^2(T) \approx 42$] and, also, when the two vortices rotate and arrange themselves along the diagonal of the square [$S/\xi^2(T) \approx 170$]. Similar effects can be observed in the curve

corresponding to $\phi/\phi_0=-12.8$ at the temperatures where one antivortex is expelled from the sample [$S/\xi^2(T) \approx 72, 79$, and 220], but not when the four antivortices are generated. The reason is that the latter is related to a smooth admixture of the LLL of irrep A with excited levels of the same irrep which, as shown in previous work on individual microstructures, does not correspond to a true phase transition between vortex states.¹⁹ The differential magnetization curves for $\phi/\phi_0=-5.25$ and -12.8 are to be compared with the one at $\phi/\phi_0=4$, which does not present any critical behavior and where we have observed a stable vortex pattern with $L=9$. Note also that in a superconducting microsquare with 20nm thickness the $\Delta M \times S / \Delta[S/\xi^2(T)]$ -amplitude in Fig. 4 will lead to magnetic moments around 10^{-15}A m^2 . Therefore these effects in the differential magnetization could be measured in arrays of 10^6 microsquares by using conventional superconducting interference device magnetometers, with a typical resolution of the order of 10^{-10}A m^2 .

IV. CONCLUSIONS

To summarize, the symmetry breaking effects in a superconducting microsquare with a magnetic dot on top strongly differ from those found in the square itself. Vorticity values forbidden at $T_c(H)$ are restored with decreasing temperature, a process which, eventually, leads to the spontaneous nucleation of vortices when cooling down the sample. This recovery of L values is associated with transitions between vortex states that can be observed experimentally in the magnetization vs temperature curves, thus opening possibilities for their study beyond those provided by local vortex imaging techniques. Other interesting aspects for the development of applications based on these properties, as their dependence on the field of the dot, deserve further studies.

ACKNOWLEDGMENTS

This work has been supported by the Research Fund K.U. Leuven GOA/2004/02, the Belgian Interuniversity Attraction Poles, and the Fund for Scientific Research Flanders (FWO). C.C. acknowledges financial support from the AQDJJ-Programme of the European Science Foundation, from Fundación Ramón Areces (Spain), and from the Ministerio de Educación y Ciencia (Spain) through MAT2004-04364.

*Email address: fmcharly@usc.es

¹W. A. Little and R. D. Parks, Phys. Rev. Lett. **9**, 9 (1962).

²D. Saint-James, Phys. Lett. **15**, 13 (1965).

³H. J. Fink and A. G. Presson, Phys. Rev. **151**, 219 (1966).

⁴V. V. Moshchalkov, Y. Bruynseraede, L. Van Look, M. J. Van Bael, and A. Tonomura, in *Handbook of Nanostructured Materials and Nanotechnology*, edited by H. S. Niiwa (Academic, San Diego, 1999), Vol. 3, Chap. 9, p. 451.

⁵V. V. Moshchalkov, L. Gielen, C. Strunk, R. Jonckheere, X. Quiu, C. Van Haesendonck, and Y. Bruynseraede, Nature (London)

373, 319 (1995).

⁶A. I. Buzdin, Rev. Mod. Phys. **77**, 935 (2005).

⁷L. F. Chibotaru, A. Ceulemans, V. Bruyndoncx, and V. V. Moshchalkov, Nature (London) **408**, 1323 (2000).

⁸J. Bonca and V. V. Kabanov, Phys. Rev. B **65**, 012509 (2002).

⁹A. S. Mel'nikov, I. M. Nefedov, D. A. Ryzhov, I. A. Shereshevskii, V. M. Vinokur, and P. P. Vyshevlavtsev, Phys. Rev. B **65**, 140503(R) (2002).

¹⁰L. F. Chibotaru, A. Ceulemans, V. Bruyndoncx, and V. V. Moshchalkov, Phys. Rev. Lett. **86**, 1323 (2001).

- ¹¹V. R. Misko, V. M. Fomin, J. T. Devreese, and V. V. Moshchalkov, Phys. Rev. Lett. **90**, 147003 (2003).
- ¹²V. A. Schweigert, F. M. Peeters, and P. S. Deo, Phys. Rev. Lett. **81**, 2783 (1998).
- ¹³V. A. Schweigert and F. M. Peeters, Phys. Rev. Lett. **83**, 2409 (1999).
- ¹⁴J. J. Palacios, Phys. Rev. Lett. **84**, 1796 (2000).
- ¹⁵G. F. Zharkov, Phys. Rev. B **63**, 224513 (2001).
- ¹⁶B. J. Baelus and F. M. Peeters, Phys. Rev. B **65**, 104515 (2002).
- ¹⁷T. Mertelj and V. V. Kabanov, Phys. Rev. B **67**, 134527 (2003).
- ¹⁸L. F. Chibotaru, G. Teniers, A. Ceulemans, and V. V. Moshchalkov, Phys. Rev. B **70**, 094505 (2004).
- ¹⁹C. Carballeira, G. Teniers, V. V. Moshchalkov, L. F. Chibotaru, and A. Ceulemans, Europhys. Lett. **75**, 936 (2006).
- ²⁰M. Morelle, J. Bekaert, and V. V. Moshchalkov, Phys. Rev. B **70**, 094503 (2004).
- ²¹L. F. Chibotaru, A. Ceulemans, M. Morelle, G. Teniers, C. Carballeira, and V. V. Moshchalkov, J. Math. Phys. **46**, 095108 (2005).
- ²²R. Geurts, M. V. Milosevic, and F. M. Peeters, Phys. Rev. Lett. **97**, 137002 (2006).
- ²³C. Carballeira, V. V. Moshchalkov, L. F. Chibotaru, and A. Ceulemans, Phys. Rev. Lett. **95**, 237003 (2005).
- ²⁴See, e.g., M. Tinkham, *Introduction to Superconductivity* (McGraw-Hill, New York, 1996), Chap. 4.
- ²⁵L. D. Landau and E. M. Lifshitz, *Electrodynamics of Continuum Media*, 2nd ed. (Pergamon, Oxford, 1984).
- ²⁶D. S. Golubovic *et al.*, Appl. Phys. Lett. **83**, 1593 (2003); D. S. Golubovic, W. V. Pogosov, M. Morelle, and V. V. Moshchalkov, Phys. Rev. B **68**, 172503 (2003); Europhys. Lett. **65**, 546 (2004); Phys. Rev. Lett. **92**, 177904 (2004); D. S. Golubovic, M. V. Milosevic, F. M. Peters, and V. V. Moshchalkov, Phys. Rev. B **71**, 180502(R) (2005).
- ²⁷L. F. Chibotaru, A. Ceulemans, G. Teniers, V. Bruyndoncx, and V. V. Moshchalkov, Eur. Phys. J. B **27**, 341 (2002).